

An integrated double half-wave organic Schottky diode rectifier on foil operating at 13.56 MHz

Kris Myny,^{a)} Soeren Steudel, Peter Vicca, Jan Genoe, and Paul Heremans^{b)}

Polymer and Molecular Electronics, IMEC vzw, Kapeldreef 75, 3001 Leuven, Belgium

(Received 16 June 2008; accepted 17 August 2008; published online 5 September 2008)

We demonstrate an integrated organic double half-wave rectifier for use in organic radio frequency identification (RFID) tags. This rectifier comprises two organic Schottky diodes, each followed by a capacitor, integrated on the same foil. This rectifier delivers approximately twice the dc voltage of single half-wave rectifiers. Its offset voltage is merely 2 V. It is able to generate voltages of 10–14 V, which are necessary for driving current organic RFID multibit code generators, from an ac-input voltage of only 8–10 V amplitude, which are generated at rf magnetic fields of 0.9–1.3 A/m. Such fields are below the minimum required rf magnetic field strength set by standards.

© 2008 American Institute of Physics. [DOI: 10.1063/1.2978348]

The field of organic thin-film transistors and circuits has gained considerable attention because of its potential for low-cost processability on flexible substrates.^{1,2} There are two main drivers in this field, being research toward radio frequency identification (RFID) tags^{3–5} and active matrix backplanes for flexible displays⁶ or sensor arrays.^{7,8} One of the key elements of an organic RFID tag is the rectifier, which yields a dc voltage from the ac-voltage detected and generated by an antenna at the targeted base carrier frequency of 13.56 MHz. This frequency is selected because it is commonly used in Si-based RFID tags, which enables partial compatibility with installed reader systems at 13.56 MHz. An important issue for organic RFID tags is the efficiency of the rectifier. A more efficient rectification will result in the required rectified dc voltage from lower ac-input voltage. This implies higher reading distances for the RFID tags. The best rectified dc voltage published for organic rectifiers⁹ is 11 V from an ac-input signal of 18 V.

A rectifier comprises diodes and capacitors. For organic diodes, two different topologies can be used, being a vertical Schottky diode^{9,10} and a transistor with its gate shorted to its drain. The transistor with shorted gate-drain node is often considered as the most favorable topology because its process flow is equal to that used for the transistors in the digital circuit of the RFID tag. In this work, however, we have chosen to use the vertical diode structure because of its better intrinsic performance at higher frequencies compared to transistors as diodes.¹¹

In a Si-based RFID tag, the supply voltage is achieved by charge pump stages, each stage comprising two diodes and two capacitors. The efficiency of a charge pump is defined by the onset voltage and the reverse leakage current of the diodes employed.¹² The higher onset voltage and the larger leakage of organic Schottky diodes make organic charge pumps inefficient and, therefore, impractical. In this letter, we propose a different approach for producing a sufficient rectified voltage for driving the digital logic on an organic RFID tag, namely, a double half-wave rectifier. We show the full integration of a plastic rectifier, based on this approach, on a flexible substrate. Furthermore, the analysis

of the performance of the integrated device allows us to get an understanding of the critical performance parameters of the diodes.

A double half-wave rectifier comprises two diodes, each followed by a capacitor. Figure 1(a) shows the schematic of this circuit. The substrate for manufacturing the rectifiers is a 200 μm thick flexible 6" polyethylenenaphtalene (PEN) foil (Teonex Q65A, DuPont Teijin Films), on which first a metal-insulator-metal (MIM) stack is processed for the capacitors in the circuit. The metal layers are 30 nm of gold and the insulator is Parylene DiX SR, with a relative dielectric constant of $\epsilon_r=3$ and a thickness of 400 nm. Conventional photolithography is used to define the capacitors in the MIM stack. Both the capacitors are 20 pF. The vertical diodes are constructed from three layers, being an anode, a semiconductor, and a cathode. The top Au layer of the MIM stack is used as anode. A 350 nm pentacene layer, the organic semiconductor, is evaporated through a shadowmask by high vacuum deposition. Last, an Al cathode is evaporated through a second shadowmask. The active area of the diodes is $500 \times 200 \mu\text{m}^2$. The described device structure is depicted in Fig. 1(c).

A double half-wave rectifier circuit comprises two single half-wave rectifiers connected between the same nodes, with diodes connected as shown in Fig. 1(a). Both single half-wave rectifiers rectify the ac-input voltage: one rectifies the upper cycles of the ac-input voltage, the other single half-wave rectifier rectifies the lower cycles of the input voltage.

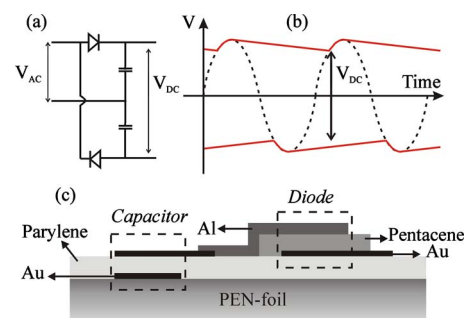


FIG. 1. (Color online) (a) Schematic of a double half-wave rectifier, (b) schematic operation of a double half-wave rectifier, and (c) vertical cross section of the integrated capacitors and diodes on foil.

^{a)}Electronic mail: kris.myny@imec.be.

^{b)}Also at E.E. Department of K.U. Leuven, Leuven, Belgium.

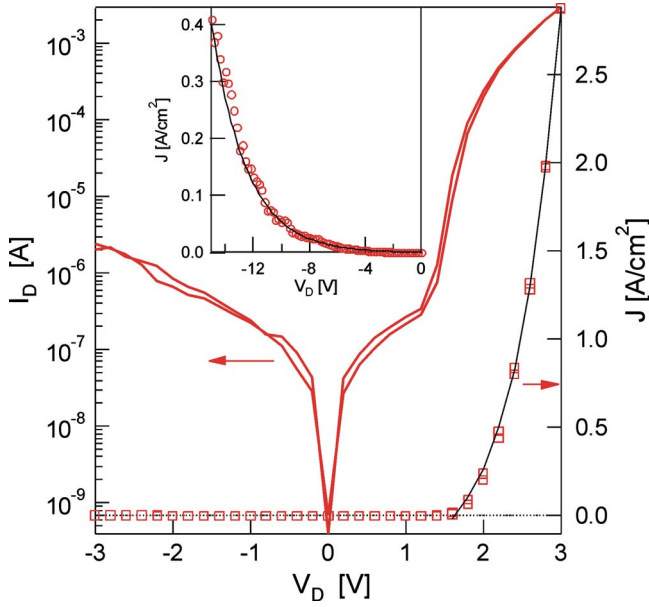


FIG. 2. (Color online) $|I|$ - V and J - V characteristics of an organic pentacene diode (area = $500 \times 200 \mu\text{m}^2$) on linear (right axis) and logarithmic (left axis) scale. The inset shows the diode leakage current density between 0 and -15 V. The fits to the data of the current densities, both in forward and in reverse biases are represented by the solid black lines.

This is schematically depicted in Fig. 1(b). The power and the ground voltage for the digital logic of the RFID tag are taken between both rectified signals [Figs. 1(a) and 1(b)]. Therefore, a double half-wave rectifier yields about double the rectified voltage compared to a single half-wave rectifier.

After the complete process of the rectifiers, the electrical behavior of a single organic diode was examined. Measurements occurred in a nitrogen-filled glovebox using an Agilent 4156C parameter analyzer. The current-voltage characteristics of a single pentacene diode are depicted in Fig. 2. The plotted characteristics show the onset voltage of the diode at about 1.2 V. However, 2 V is required to obtain a current beyond 200 mA/cm^2 . At a 3 V forward bias, the current density is 2.88 A/cm^2 . The leakage current of the diode shows an important increase when the reverse bias increases, limiting the maximum reverse voltage over the diode.

For ac measurements of the rectifiers, we constructed a small printed circuit board (PCB), comprising coax connections for the ac-input signal and the dc output signal. The ac signal is terminated with 50Ω for limiting reflections at 13.56 MHz. The dc signal is sent to the oscilloscope (MSO6014A of Agilent Technologies) on which the dc voltage was read out, having an input impedance of $1 \text{ M}\Omega$, which is the load of the rectifier. The rectifier foil is placed into a socket which is plugged in the PCB. We used a Si-based double half-wave rectifier circuit (assembly of 1N4148 diodes and 20 pF capacitors) as a reference. Figure 3 plots the rectified dc voltage of the integrated organic and assembled Si-based rectifiers versus the ac-input voltage at a frequency of 13.56 MHz, which is the target frequency for organic RFID tags. At an amplitude of the ac voltage of 10.9 V, the rectified dc voltage of the organic rectifier is 14.9 V, while the Si-based rectifier produces 20.6 V. The slope of the measured V_{dcout} as a function of applied V_{acin} , which we term the efficiency of the rectifier, is 1.64 for the organic rectifiers and 2 for the silicon diodes. The onset voltage of the diodes

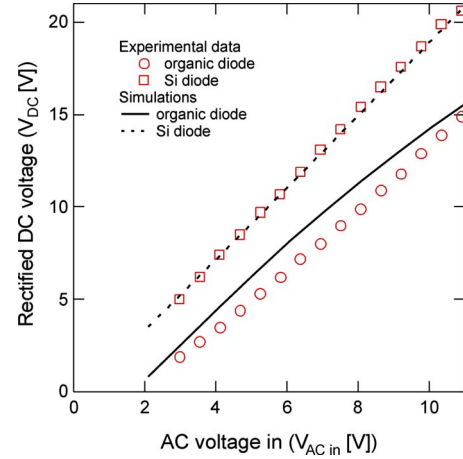


FIG. 3. (Color online) Simulation results and experimentally obtained data points of the rectified dc output voltage vs the ac-input voltage for an organic rectifier and a Si-based rectifier both in double half-wave rectifier configuration.

can be estimated by extrapolation to an output voltage of 0 V and is 1.98 V for the organic rectifier and 0.42 V for the silicon rectifier. Each organic diode, therefore, has an onset voltage of only about 1 V.

To get a better understanding of the efficiency limitations of the organic rectifier, in particular the slope efficiency of $V_{\text{dcout}}/V_{\text{acin}} = 1.64$, we model the behavior of the circuit in Fig. 1 using the characteristics in Fig. 2. Both the forward and the reverse current density J can be expressed quite accurately as a function of the voltage V using the exponential curve $J(V) = J_0 + J_1 \exp(\alpha V)$. In the relevant forward current range (1.6 to 3 V, see Fig. 2), $J_0 = -0.311 \text{ A/cm}^2$, $J_1 = 0.0189 \text{ A/cm}^2$, and $\alpha = 1.71 \text{ V}^{-1}$. In the relevant reverse current range (-15 to -1 V, see inset Fig. 2), $J_0 = 0 \text{ A/cm}^2$, $J_1 = 0.001 \text{ A/cm}^2$, and $\alpha = -0.4 \text{ V}^{-1}$. These fits, extracted from the quasistatic characteristics, have been used to calculate the output voltage (V_{dc}) as a function of the ac-input amplitude (V_{in}) by numerical matching the charging and discharging currents of the rectifier's capacitor using Eq. (1), derived from the equations and conditions outlined in Ref. 9,

$$\begin{aligned} & \frac{1}{2\pi} \int_{\pi - \sin^{-1}(V_{\text{dc}}/2V_{\text{in}})}^{2\pi + \sin^{-1}(V_{\text{dc}}/2V_{\text{in}})} J \left(V_{\text{in}} \sin(\theta) - \frac{V_{\text{dc}}}{2} \right) \partial \theta + \frac{V_{\text{dc}}}{2AR_L} \\ &= \frac{1}{2\pi} \int_{\sin^{-1}(V_{\text{dc}}/2V_{\text{in}} + 1.6/V_{\text{in}})}^{\pi - \sin^{-1}(V_{\text{dc}}/2V_{\text{in}} + 1.6/V_{\text{in}})} J(V_{\text{in}} \sin(\theta) - V_{\text{dc}}/2) \partial \theta, \end{aligned} \quad (1)$$

with A being the device area (0.001 cm^2) and R_L being the load resistance ($1 \text{ M}\Omega$). For the commercial silicon diode, the curves from the datasheet have been used.¹³

Figure 3 compares the calculated output voltage with the measured voltage. The slope efficiency is almost exactly reproduced. We can now trace back the origin of the slope efficiency to the presence of the reverse leakage current of the organic diodes: at higher input voltages, the leakage current increases exponentially, which discharges the capacitors, resulting in a lower dc output voltage. On the other hand, the modeled curve overestimates the dc output voltage by approximately a constant amount of 1 V, or 0.5 V for each diode. This has not been elucidated at present, and could be

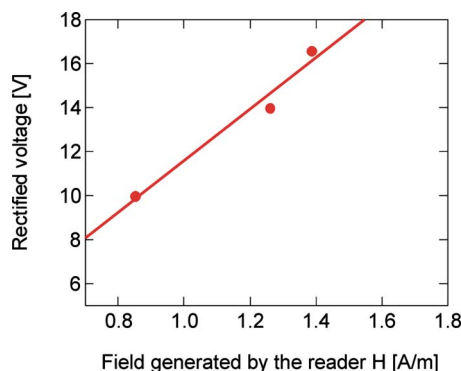


FIG. 4. (Color online) Internal rectified voltage of a double half-wave rectifier generated in an organic RFID tag vs the 13.56 MHz magnetic field generated by the reader.

attributed to several factors, for example, a slightly higher offset voltage or a slightly degraded mobility of the charge carriers by bias stress during the prolonged measurement time. We conclude from this analysis that the efficiency of the rectifier depends on the on/off ratio of the diode current.

The organic double half-wave rectifier is also examined as a part of a fully organic RFID tag at 13.56 MHz. Details of the full tag are published elsewhere.⁵ This RFID tag comprises an *LC* antenna, fabricated on two foils, a double half-wave rectifier foil, and a multibit transponder foil including an integrated load modulator. All foils are placed into a socket and connected to each other using a PCB. The RFID reader is a 7.5 cm radius antenna, which emits the field at a base carrier frequency of 13.56 MHz. In Fig. 4, the internal rectified voltage of this double half-wave rectifier in the organic RFID tag is plotted as a function of the field generated by the reader, for the tag antenna placed in the near field of the reader antenna, at a distance of about 4 cm from the coil generating the reader's 13.56 MHz rf field. As can be seen in the graph, 10 V rectified voltage is obtained at a 13.56 MHz electromagnetic field of about 0.9 A/m, and 14 V at 1.26 A/m. The latter is the voltage currently required by our organic transponder chips.⁵ The ISO 14443 standard states that RFID tags should be operational at a minimum required rf magnetic field strength of 1.5 A/m. The double half-wave rectifier circuit presented here therefore satisfies this ISO norm. After extrapolation of the measurement data, a dc voltage of 17.4 V can be obtained at a field of 1.5 A/m. If a single half-wave rectifier was used, the rectified voltage

would be limited to 8–9 V, which is too low for current organic technology.

To summarize, in this work we demonstrated an integrated rectifier circuit for the use in organic RFID tags, being a double half-wave rectifier. It comprises two diodes, each followed by a capacitor. This rectifier delivers about double the dc voltage of a single half-wave rectifier. The rectifier readily generates the supply voltage needed for driving current multibit code generators of organic RFID tags when placed in the near field of a standard reader antenna powered below the minimum required rf magnetic field strength of 1.5 A/m, set by standards. Our measurements show that the full integration of the rectifier on foil does not compromise its performance. Finally, we show that the main bottleneck today is the reverse leakage current, which limits the slope efficiency of this rectifier.

This work was performed in a collaboration between IMEC and TNO in the frame of the HOLST Centre. Part of this work was supported by the European-funded Integrated Project POLYAPPLY (IST No. 507143).

¹H. Klauk, M. Halik, U. Zschieschang, F. Eder, G. Schmid, and C. Dehm, *Appl. Phys. Lett.* **82**, 4175 (2003).

²T. Sekitani, Y. Kato, S. Iba, H. Shinaoka, T. Someya, T. Sakurai, and S. Takagi, *Appl. Phys. Lett.* **86**, 073511 (2005).

³P. F. Baude, D. A. Ender, M. A. Haase, T. W. Kelley, D. V. Muyres, and S. D. Theiss, *Appl. Phys. Lett.* **82**, 3964 (2003).

⁴E. Cantatore, T. C. T. Geuns, G. H. Gelinck, E. van Veenendaal, A. F. A. Gruijthuijsen, L. Schrijnemakers, S. Drews, and D. M. de Leeuw, *IEEE J. Solid-State Circuits* **42**, 84 (2007).

⁵K. Myny, S. Van Winckel, S. Steudel, P. Vicca, S. De Jonge, M. J. Beenhakkers, C. W. Sele, N. A. J. M. van Aerle, G. H. Gelinck, J. Genoe, and P. Heremans, *IEEE ISSCC Dig. Tech. Papers*, pp. 290–291 (2008).

⁶G. H. Gelinck, H. E. A. Huitema, E. van Veenendaal, E. Cantatore, L. Schrijnemakers, J. B. P. H. van der Putten, T. C. T. Geuns, M. Beenhakkers, J. B. Giesbers, B.-H. Huisman, E. J. Meijer, E. M. Benito, F. J. Touwslager, A. W. Marsman, B. J. E. van Rens, and D. M. de Leeuw, *Nat. Mater.* **3**, 106 (2004).

⁷T. Someya, T. Sekitani, S. Iba, Y. Kato, H. Kawaguchi, and T. Sakurai, *Proc. Natl. Acad. Sci. U.S.A.* **101**, 9966 (2004).

⁸T. Someya, Y. Kato, T. Sekitani, S. Iba, Y. Noguchi, Y. Murase, H. Kawaguchi, and T. Sakurai, *Proc. Natl. Acad. Sci. U.S.A.* **102**, 12321 (2005).

⁹S. Steudel, K. Myny, V. Arkhipov, C. Deibel, S. De Vusser, J. Genoe, and P. Heremans, *Nat. Mater.* **4**, 597 (2005).

¹⁰B. N. Pal, J. Sun, B. J. Jung, E. Choi, A. G. Andreou, and H. E. Katz, *Adv. Mater. (Weinheim, Ger.)* **20**, 1023 (2008).

¹¹S. Steudel, S. De Vusser, K. Myny, M. Lenes, J. Genoe, and P. Heremans, *J. Appl. Phys.* **99**, 114519 (2006).

¹²F. Pan and T. Samaddar, *Charge Pump Circuit Design*, 1st ed. (McGraw-Hill, New York, 2006).

¹³1N4148, General Semiconductor.